Red Blood Cell Velocity Measurement of Rodent Tumor Model：An in vivo Microscopic study

Wen-Chen Lin[1], Chih-Chieh Wu[2], Ren-Shyan Liu[3,4], Tzung-Chi Huang[5,*], Kang-Ping Lin[1,*]

[1]Department of Electrical Engineering, Chung Yuan Christian University, Taiwan

[2]Instrument Technology Research Center, National Applied Research Laboratories, Taiwan

[3]Department of Biomedical Imaging and Radiological Sciences, National Yang-Ming University, Taiwan

[4]Department of Nuclear Medicine, Taipei Veterans General Hospital, Taiwan

[5]Department of Biomedical Imaging and Radiological Science, China Medical University, Taiwan

[*]Corresponding author: tzungchi.huang@mail.cmu.edu.tw (T.-C. Huang), kplin@cycu.edu.tw (K.-P Lin)

Abstract

Blood flow dynamics in micro-vessels of small animal tumor model provide important physiological and pathological information. In this study, red blood cell velocity in micro-vessels that distributed near the surface of rodent tumor model was investigated using an approach on the basis of optical flow estimation. A long-term experiment was performed to observe tumor growth on nude mice and to monitor the variation of blood flow velocity. The blood flow images were acquired by a capillaroscopy, M320 (JMC Corporation, Kyoto, Japan), with a spatial resolution of 1.42 μm and an image sampling rate of 30 frames per second. Frame to frame image registration with mutual information feature matching was used to stabilize images by which vessel shift problem resulted from regular heartbeats can be eliminated. The blood flow results measured by optical flow method have compared with visual inspection to valid the accuracy. The blood flow observation in this study was focused on the tumor surface of nude mice. Multiple weekly data were acquired from each nude mouse for five weeks after tumor implantation. The averaged red blood cell velocities of capillaries were measured and calculated at different weeks for each tumor. The distribution of blood flow velocity among all samples was ranged from 40 to 350 μm/s. The differences in vessel diameter and blood flow velocity during tumor growth were studied in comparison with the initial week. According to the obtained p value ($p<0.05$) of data, significant difference can be found between the velocity values at the initial week and the 2nd week. The results by using the presented imaging system and analysis method suggested an optical based process has the potential to develop new experimental protocols in numerical simulation of tumors growth. This measurement system may also be useful in many other biotechnological evaluations.

Keywords: Microcirculation, Blood flow velocity, Tumor growth

Introduction

Microcirculation has known to be a crucial factor in maintaining healthy tissues and functional organs because of its functions of delivering oxygen and nutrients. Nowadays, the relationship between blood flow in microcirculation and the clinical physiology in blood circulation has been widely discussed in many researches. In addition, studies showed that various risk factors of disease can be related to corresponding changes in microcirculation. For instance, Raynaud's syndrome [1, 2], hypertension [3, 4] and diabetes [5, 6] are usually accompanied with impaired microcirculation. Therefore, microcirculation information, which consists of vessel diameter, flow velocity, vessel density, permeability, leucocyte function, and tracer appearance times, plays an important role in health assessment and angiopathy prevention. In order to identify the characteristics of microcirculation in illness and its relationship in response to medicinal drugs, the hemodynamic characteristic of blood flow [7-9] is one of the essential factors. An atypical characteristic was found that the advance of the heterogeneous nature of blood flow in tumors would result in lack of nutrient supplement to tissues. Although there have been hypotheses established, further investigations are still needed to thoroughly explain the actual mechanisms of this bizarre characteristic in tumor microcirculation. [10]. The measurement of blood flow velocity at local micro-vessels is one of effective ways to observe and quantify the micro-vessel differences during tumor growth. Several studies were published focusing on tumor microcirculation using intravital video microscopy (IVVM) to allow dynamic observation of red blood cell (RBC) activity in the microcirculation of intact organs and tissues in live animals, such as laboratory mouse [4, 5]. Even though blood flow in large vessels is able to be measured by using electro-magnetic blood flowmeter or ultrasonic Doppler flowmeter, measuring the flow of RBC in micro-vessels is still a challenge. A major limitation of such measurements has been their inability to relate micro-vascular perfusion observed within individual micro-vessels to the topographical succession of arterioles, capillaries, and venules peculiar to a given tissue. The image

velocimetry procedure, which is based on the distribution of the apparent velocities of movement of a brightness pattern in an image, is applied to analyze the distribution of velocities in an arterial bifurcation under steady blood flow conditions. This is a non-contact procedure that could further be applied to analyze the cyclic variation of the pulsatile blood flow through a micro-vessel in the absence of the electrogastrogram (EGG), and from a sequence of recorded images covering more than one flow cycle [11].

Previously we successfully developed the optical instrument and the method for analysis micro-vascular blood flow [12]. The purpose of this study is to observe the temporal heterogeneity in tumor blood flow applying our previously established system. The blood flow observations in this study were focused on the tumor surface in nude mice. Multiple data were obtained weekly from each nude mouse for 5 weeks after tumor implantation.

Materials and Method

Animal preparation

7– 12 weeks old male nude mice with severe combined immune deficiency (SCID), and with an average weight of 22g, were used for tumor blood flow measurements and vital microscopic observations under anaesthesia. The SCID mice were injected subcutaneous tumors (2×10^6 cells in 0.05 ml) under the skin of the rear dorsum, housed in groups of two in a standard cage at 21 °C in a 12 h dark/12 h light cycle and supplied with laboratory chow and distilled water. The mice were randomly allocated into five groups to observe micro-vascular blood velocity on the tumor surface for five weeks. Experimental setup were illustrated in Fig. 1 (a).

In surgical preparation, the mice were anesthetized with pentobarbital. The intraperitoneal induction dose used was 70 mg/kg of body weight. The animals were laid sideways on an operating table; surface temperature of body was kept at

36.5-37.5 °C by a heat lamp. The skin area was carefully incised and separated 2-2.5 cm long for microcirculation observation on the surface of the solid tumor (Fig. 1 (b)). After measurements, the skin incision was closed by a suture. At the end of the experiment, these animals were killed by an overdose of pentobarbital.

Capillaries Microcirculation on Nude Mice

Microcirculation covers blood flows in arterioles, capillaries and venules. The capillaries connect the arterioles with venules. Capillaries are not only the smallest but also greatest in amount of blood vessels in human body The extensive branching networks dramatically increase the surface areas for the rapid exchange of molecules. capillaries are small diameter vessels allowing only one RBC to pass. Among which, the ones connect arteries are known as pre-capillary. Pre-capillaries are vessels about 3~5 times of capillaries in diameter lack complete coats. Except for what mentioned above, they don't have much difference from capillaries in other aspects. Moreover, the density of capillary microcirculation on tumor surfaces of mice were observed, imaged and displayed by using the microscopic system without fluorescently labeling, as shown in Fig 1 (c)-(e).

Microscopy and Imaging acquisition

Our microscopic system without fluorescently labeling provides precise and continuous quantitative data of blood flow rate in individual small vessel. The wavelength and illumination are key parameters of the light source in a microcirculation imaging system. The microcirculation was imaged by the penetrating green channel of white light from the side. Hemoglobin of erythrocytes absorbed green channel of white light therefore was observed as dark moving cells. The image was projected by magnifying lens onto a camera. The imaging light, collected by the central part of the light

guide, was optically isolated from the illuminating white light from the light-emitting diodes (LEDs). These LEDs were arranged in circle at the tip of the light guide, which directly illuminated the area of interest (Fig. 2). The technique of window scanning was used in this application. This commonly used technique can also be applied in horizontal, vertical or diagonal pixels scans, and is efficient for sampling spatial information on a tumor surface. A comparison of the two scanning orientations, horizontal and vertical, was performed in this study. The scan in either orientation moved on the constructed geometry signature by a distance of 1mm per line. In this study, the image pixel matrix was up to 720 × 480 pixels.

Imaging Processing and RBC velocity

Respiration and pulsatile heartbeats result in oscillatory movement of the body in intravital microscopy system. Therefore, image stabilization was the first step of image processing. With a cost (or similarity) function to quantify the quality of the alignment of the two images, frame-to-frame image matching is an effective solution to the motion problem [12]. The procedures prior to the implementation of optic flow algorithm were to process each pair of digitized images by homomorphic filtering, median filtering, and finally matching filter. Tereafter the modified optical flow algorithm was implemented in Microsoft (MS) Visual C++™. Therefore, the preprocessing of images has some advantages stated below:

Homomorphic filtering. Since the videomicroscopic images of blood flow through microvessels were low contrast, we focused on the improvement of grey-level images using a homomorphic filter which provided good dynamic range compression and contrast enhancement [13].

Median filtering. The image recoding systems still need to be improved to avoid the image contamination by noise to various levels though it may or may not be visible. Median filtering is a nonlinear operation that is implicitly edge-adaptive.

Using a 5×5 window-sized median filter could denoise the image by reducing the blurring of edges.

Matching filter. According to the theory described in former research, the vascular images were calculated by a simplistic matched filter after Gaussian smoothing in order to ease the computation and to segment microvessel tree. [14]. Vessel density can be calculated as the number of vessels crossing the lines divided by the total length of the lines.

Velocity estimation. A gradient-based deformable image registration algorithm, the optical flow method (OFM) [15, 16], was applied to calculate the RBC velocity on two successive images. In our previous study, an automatic RBC velocity estimation system was developed to performed OFM-based measurement of RBC velocity in a complete, clip-shape capillary [12]. The flowchart of velocity estimation is demonstrated in Fig. 3. Based on Horn and Schunck method, we develop an approach to constrain optical flow field. For Horn and Schunck method, it calculates optical flow within gradient of images by iterating the equation 1.

$$\hat{v}_x^{(k+1)}(X,t)=\bar{v}_x^{(k)}(X,t)-\frac{\partial f}{\partial x}\left(\frac{\frac{\partial f}{\partial x}\cdot\bar{v}_x^{(k)}(X,t)+\frac{\partial f}{\partial y}\cdot\bar{v}_y^{(k)}(X,t)+\frac{\partial f}{\partial t}}{\alpha^2+\left(\frac{\partial f}{\partial x}\right)^2+\left(\frac{\partial f}{\partial y}\right)^2}\right)$$

$$\hat{v}_y^{(k+1)}(X,t)=\bar{v}_y^{(k)}(X,t)-\frac{\partial f}{\partial y}\left(\frac{\frac{\partial f}{\partial x}\cdot\bar{v}_x^{(k)}(X,t)+\frac{\partial f}{\partial y}\cdot\bar{v}_y^{(k)}(X,t)+\frac{\partial f}{\partial t}}{\alpha^2+\left(\frac{\partial f}{\partial x}\right)^2+\left(\frac{\partial f}{\partial y}\right)^2}\right) \qquad \text{(eq 1)}$$

where *k* is the iteration counter, the overbar denotes weighted local averaging (excluding the present pixel), and all partials are evaluated at the point (x, y, t). The initial estimates of the velocities $v_x^{(0)}(X,t)$ and $v_y^{(0)}(X,t)$ are usually taken as zero. If objects movement is large or no features are overlapping, the Horn and Schunck optical flow method could not have a reliable velocity flow field. To avoid this problem, we reprocess the Horn and Schunck optical flow with a deformed image which is depending on the velocity field we have estimated from source image. By this way, we could modify features to the covered pattern according to the correct patterns in the next frame. It would correct some information for

motion estimation and help to get a suitable velocity field. In another study, we discussed the use of three techniques in RBC velocity measurement with simulated blood flow images [22-25]. OFM, space-time diagram (Hough transform based estimation) and cross-correlation method (CCM) are feasible and common solutions for RBC velocity determination. Among those three approaches, OFM demonstrates the highest accuracy in RBC velocity calculation with simulated blood flow patterns of micro-vessels. Velocity estimation was based on analyzing intensity variation of pixels on the skeleton of vessel. A thinning method [12], which enables a continuous vessel skeleton including small and large micro-vessels, was applied on the vascular tree segmentation. The obtained skeleton was independent of the position of region of interest (ROI) on an image pixel matrix of 256 × 256. Thus, the measurements of RBC velocity are consistent and reproducible (Fig. 4).

Results and Discussion

Tumors in mice

A total of 25 mice which weighed about 22.7 ± 0.88 g, were divided into two groups. Ten mice were in the control group while the other 15 were in the tumor experimental group. Fig. 5 shows the weekly tumor growth on the back leg muscle of SCID mice. Table 1 lists the average sizes measured every week in the experiment group after tumor implantation. Fig. 6 shows the weekly average volumes. Tumors grew gradually in the first 2 weeks with mild rates of 49.58 mm^3 in the 1^{st} week and 63.37 mm^3 in the 2^{nd}. The growth was rapid in the 3^{rd} (228.22 mm^3) and 4^{th} weeks (470.45 mm^3) but slowed down in the 5^{th} (503.50 mm^3). This weekly measurement data agree with typical tumor growth pattern which is defined by 3 phases: initial, growth and late phases.

The blood vessel diameters on the surface of the tumors were measured weekly during the experiment (Fig. 7). Several studies using IVVM technique to measure the velocity distribution in blood vessels with a diameter of 20–30 μm

showed the presence of a heartbeat in the vessels [17]. In this study, any vessel with a diameter smaller than 30 μm was defined as a small vessel while the one larger than 30 μm was defined as a large vessel. The size of both small and large vessels did not change substantially in the first 4weeks with the average diameter of small vessels remained in 21μm . In the 5th week ; however, a noticeable growth of 6μm was shown and the average diameter reached to 27μm. As to large vessels, significant increase of growth appeared in the 4th week. This group of vessels exhibited a 13μm difference in diameter comparing to an average of 38μm in the first 3weeks and the subsequently 51μm in both the 4th and 5th week.(Table 2). The result also showed differences between the initial and the late phase of the large vessels were about twice of the difference of the small vessels.

Blood flow velocity

The microcirculation blood flow velocity data on tumor surface is displayed in Table 2 and Fig. 8. In general, the blood flow velocities were between 40 and 350 μm/s varying with mouse and tumor area. For the experimental case in the initial week (week 0), the blood flow velocity in the large vessels was always faster than that in the small vessels. The average velocity was 150.54 ± 32.28 μm/s for the large vessels and 112.74 ± 57.62 μm/s for the small vessels. In the tumor case of experimental group, for both large and small vessels, the highest flow velocity was found in the 2nd week and the 1st week is the second. The average of the highest velocity was 171.76 ± 82.22 μm/s for the small vessels and 198.84 ± 58.79 μm/s for the large vessels. The second highest velocity were 131.20 ± 23.72 μm/s and 171.25 ± 98.07 μm/s in average of small vessels and large vessles respectively. However, the small and large vessels presented an opposite tendency from the 3rd to the the 5th weeks. In small vessels, the blood flow gradually declined through the last 3 weeks. The average values for the small vessels from the 3rd to the 5th weeks were 130.92 ± 59.52, 126.96 ± 49.87 and 110.67 ± 63.20 μm/s accordingly.

Whereas, in the large vessels, the velocity had a sudden decrease in the 3rd week, it rose gradually in the last 3weeks. But the velocities did not exceed which of the first two weeks. The values for the large vessels in the 3rd through the 5th weeks were 116.95 ± 46.71, 130.20 ± 56.30 and 148.37 ± 55.46 μm/s accordingly. Statistical analysis of blood flow velocity was done by independent T test. According to the obtained p value ($p<0.05$) of data in each week to week 0, significant difference can be found between the velocity values at 2nd week. In the experimental group, significant difference ($p<0.01$) can be found between the vessel diameter values in each week. The blood flow velocity in the large vessels was larger than that in the small vessels with an exception of the 3rd week. Since the definition of arteriolar or venular are not suitable to describe vessels in tumors, we do not use those terms in this article[18]. Briefly, our results obtained by the presented imaging system and analysis method were in close consistency to the literature [19]. In their study, the blood flow velocity measured at the tumor surface of SCID mice was approximately 200 μm/s with a range of 0~600 μm/s.

Discussion

Based on the above, the differences in vessel diameter and blood flow velocity during tumor growth were found to be statistically significant. The blood vessel density increases with the tumor growth, reaches the highest at the late phase [20, 21]. According to the observed tumor growth curves in our experiment, tumors grew from none to some volumes in the initial phase (the 1st and 2nd weeks). The regional nutrition and oxygen requirement in the initial phase would be high. To satisfy this high demand, the incomplete microcirculation system in the initial phase was compensated with high blood flow velocity. In the growth phase (the 3rd and 4th weeks), the slow blood flow in tumor microcirculation was a result of the following two facts. First, the micro-vessels in tumor tissues are different from those in normal tissues. In tumor tissues, the micro-vessels are lumens formed by a layer of endothelial cells as barrier walls. These lumens have the characteristics of incomplete differentiation, and are not controlled by nerves, which causes the condition of paralysis to the micro-vessels.

The blood flow in such micro-vessels hence cannot be varied by varying the diameter, and the flow velocity in such a vessel tends to be constant. Second, the high density microcirculation system is well established in this phase, which can provide sufficient nutrition and oxygen to the tumor cells even with a relatively slow blood flow. In the 4^{th} and 5^{th} weeks, tumor growth is still fast. The cells in the edge regions usually acquire more nutrition and oxygen than those in the tumor center. As the micro-vessels are lower in density or even not present in the center volume, the blood flow velocity stop increasing. As a result, apoptosis is often found in the tumor cells in the center volume due to ischemia. Finally, the distinctions from the previous researches are emphasized as follows. In several experimental methods, using intravital microscopy techniques with fluorescently labeling have been used to measure temporal instabilities in red blood cell flow in individual vessels in small sub-regions of tumors growing in window chambers. However, some detrimental effects may arise with fluorescence microscopy on living tissues. For long-term observation, this study was carried out a microscopy system without fluorescence to evaluate the velocity range of blood flow through a solid tumor area. With the results of a valid model, we could further develop new experimental protocols in numerical simulation of tumors growth.

Conclusion

A microcirculation imaging system, which uses white-light LED as the illuminant light source and without fluorescently labeling, was applied in this study. This system was used in the in vivo tumor surface microcirculation blood flow velocity measurement on small animals. With the application of dynamic image processing on series of microcirculation images, and a blood flow velocity calculation algorithm, weekly blood flow velocity data were collected from the tumor surface micro-vessels in nude mice. The techniques used in this microcirculation study have the potential in the applications of tumor development evaluation and prognosis. The tumor microcirculation data of small animals

obtained in this study could be a reference in the future tumor and blood pathophysiology research.

Acknowledgments

The authors acknowledge with gratitude the financial support granted by the National Research Program for Genomic Medicine (Molecular and Genetic Imaging Core, NSC99-3112-B-010-015), the National Science Council (NSC) research grant (NSC99-2221-E-033-012-MY3) and the Department of Industrial Technology (DoIT) of the Ministry of Economic Affairs (MOEA) (99-EC-17-A-19-S1-163), Taiwan.

References

[1] Bertuglia S., Leger P., Colantuoni A., Coppini G., Bendayan P. and Boccalon H. Different flowmotion patterns inhealthy controls and patients with Raynaud's phenomenon Technol, Health Care 7 113–23, 1999.

[2] Wollersheim H., Reyenga J. and Thien T . Laser Doppler velocimetry of fingertips during heat provocation in normals and in patients with Raynaud's phenomenon Scand, J. Clin. Lab. Invest. 48 91–5, 1988.

[3] Cesarone M R, Incandela L, Ledda A, De Sanctis M T,Steigerwalt R, Pellegrini L, Bucci M, Belcaro G andCiccarelli R. Pressure and microcirculatory effects of treatment with lercanidipine in hypertensive patients and invascular patients with hypertension. Angiology 51 53–63, 2000.

[4] Cesarone M R, Laurora G and Belcaro G V. Microcirculation in systemic hypertension. Angiology 43 899–903,1992.

[5] Hudetz A, Feher G, Weigle C, Knuese D and Kampine J . Video microscopy of cerebrocortical capillary flow: response to hypotension and intracranial hypertension Am. J. Physiol.268 2202–10, 1995.

[6] Rayman G, Hassan A and Tooke J E . Blood flow in the skin of the foot related to posture in diabetes mellitus Brit. Med. J. 292 87–90, 1986.

[7] Katsuyoshi Hori, March Suzuki , Shigeru Tanda, Sachiko Saito . Characterization of Heterogeneous Distribution of Tumor Blood Flow in the Rat. Cancer Science. Volume 82 Issue 1, pp. 109 – 117, 1991.

[8] Francesco Mollica, Rakesh K. Jain and Paolo A. Netti. A model for temporal heterogeneities of tumor blood flow. Microvascular Research. Volume 65, Issue 1, Pages 56-60, 2003.

[9] Arthur M. Iga, Sandip Sarkar, Kevin M. Sales, Marc C. Winslet and Alexander M. Seifalian, Quantitating Therapeutic Disruption of Tumor Blood Flow with Intravital Video Microscopy, Cancer Research 2006; 66: (24). December 15, 2006.

[10] James W. Baish, Paolo A. Netti, and Rakesh K. Jain. Transmural Coupling of Fluid Flow in Microcirculatory Network and Interstitium in Tumors. Microvascular Research 53, pp. 128–141, 1997.

[11] M. Manjunatha, Swaroop S. Singh, Megha Singh. Blood flow analysis in mesenteric microvascular network by image velocimetry and axial tomography. Microvascular Research, Volume 65, Issue 1, pp.49-55, 2003.

[12] Chih-Chieh Wu, Geoffrey Zhang, Tzungchi Huang, Kang-Ping Lin, Red blood cell velocity measurements of complete capillary in finger nail-fold using optical flow estimation. Microvascular Research, (78)319-324, 2009.

[13] Holger G. Adelmann. Butterworth equations for homomorphic filtering of images. Computers in Biology and Medicine, Volume 28, Issue 2, pp. 169-181, 1998.

[14] George K. Matsopoulos, Nicolaos A. Mouravliansky, and et al.. Automatic Retinal Image Registration Scheme Using Global Optimization Techniques. IEEE Transactions on Information Technology in Biomedicine, Vol. 3, no. 1, 1999.

[15] Zhang G, Huang T-C, Guerrero T, et al. Use of three-dimensional (3D) optical flow method in mapping 3D anatomic structure and tumor contours across four-dimensional computed tomography data. J Appl Clin Med Phy 9, 59-69 , 2008.

[16] Zhang G, Huang T-C, Forster K, et al. Dose mapping: validation in 4D dosimetry with measurements and application in radiotherapy follow-up evaluation. Comp Meth Prog in Biomed. 90, 25-37, 2008.

[17] Jae Hong Jeong, Yasusiko Sugii, Motomu Minamiyama, Koji Okamoto. Measurement of RBC deformation and velocity in capillaries in vivo. Microvascular Research 71, pp. 212–217, 2006.

[18] Eddy HA, Casarett GW. Development of the vascular system in the hamster malignant neurinom. Microvascular Research 6, pp.63-82, 1973.

[19] Torres Filho IP, Leunig M, Yuan F, Intaglietta M, Jain RK. Noninvasive measurement of microvascular and

interstitial oxygen profiles in a human tumor in SCID mice. Proc. Natl. Acad. Sci. USA. 91(6):2081-5, 1994.

[20] Jie Wu, QuanLong, ShixiongXu, AnwarR.Padhani. Study of tumor blood perfusion and its variation due to vascular normalization by anti-angiogenic therapy based on 3D angiogenic microvasculature. Journal of Biomechanics 42, pp.712–721, 2009.

[21] Dai Fukumura, Rakesh K. Jain. Tumor microvasculature and microenvironment: Targets for anti-angiogenesis and normalization. Microvascular Research, Volume 74, Issues 2-3, pp.72-84, 2007.

[22] T-C Huang, W-C Lin, C-C Wu, G. Zhang, K-P Lin. "Experimental estimation of blood flow velocity through simulation of intravital microscopic imaging in micro-vessels by different image processing methods," Microvascular Research, 80(3), pp.477-483, 2010.

[23] C-C Wu, G. Zhang, T-C Huang, K-P Lin. "Red blood cell velocity measurements of complete capillary in finger nail-fold using optical flow estimation," Microvascular Research, 78, pp.319-324, 2009.

[24] T-C Shih, G. Zhang, C-C Wu, H-D Hsiao, K-P Lin, T-H Wu, T-C Huang. "Hemodynamic analysis of capillary in finger nail-fold using computational fluid dynamics and image estimation," Microvascular Research, 81, pp.68-72, 2010.

[25] C-C Wu, W-C Lin , G. Zhang, C-W Chang, R-S Liu, K-P Lin, T-C Huang. "H Accuracy evaluation of RBC velocity measurement in nail-fold capillaries," Microvascular Research, doi:10.1016/j.mvr.2011.01.003 (2011).

Table 1 Tumor dimensions and volume (Mean ±SD), n is vessel number

	1st week (n=17)	2nd week (n=17)	3rd week (n=17)	4th week (n=17)	5th week (n=17)
Length (mm)	6.24 ± 0.43	7.35 ± 2.23	11.59 ± 3.66	12.39 ± 0.03	12.49 ± 0.67
Width (mm)	5.77 ± 0.25	6.12 ± 0.41	8.14 ± 0.48	11.27 ± 0.93	11.07 ± 0.56
Higth (mm)	1.37 ± 0.15	1.45 ± 0.33	2.53 ± 0.67	3.40 ± 0.62	3.65 ± 0.21
Volume (mm^3)	49.58 ± 10.26	63.37 ± 13.50	228.22 ± 45.66	470.45 ± 45.57	503.50 ± 27.59

Table 2 Vessel diameter and blood flow velocity in tumor micro-vessels (Mean ±SD), n is vessel number

		Week 0 (n=26)	1st week (n=17)	2nd week (n=17)	3rd week (n=17)	4th week (n=17)	5th week (n=17)
diameter	≦30μm	17.34 ± 5.86	22.68 ± 4.24	20.51 ± 6.18	21.31 ± 4.78	20.30 ± 5.17	27.03 ± 2.53
	＞30μm	38.41 ± 2.41	38.35 ± 7.41	38.17 ± 4.61	38.03 ± 3.29	52.43 ± 15.16	50.52 ± 16.87
velocity (um/s)	≦30μm	112.74 ± 57.62	131.20 ± 23.72	171.76 ± 82.22	130.92 ± 59.52	126.96 ±49.87	110.67 ± 63.20
	＞30μm	150.54 ± 32.28	171.25 ± 98.07	225.35 ± 66.63	116.95 ± 46.71	130.20 ± 56.34	148.37 ± 55.46

Legend

Fig.1 (a)Experimental setup. White light microscopic system without fluorescently labeling M320 (JMC Corporation, Kyoto, Japan) using a closed-circuit video system consisting of a CCD video camera, a LCD monitor, and a video recorder. Video recorder acquires real-time blood flow video of microcirculation at ×380 magnification, with a spatial resolution of 1.42μm and image sampling rate of 30 frames per second. The static image pixel size is 720×480. (b) left : animal preparation. .Tumor cells implantation was within the dotted line rectangle in the nude mouse with SCID. (b) right : the microcirculation in the tumor region observed after an easy surgery of surface treatment. The microcirculation of capillaries on nude mice is observed as shown in this illustration. Various densities of micro-vessels are shown, such as (c) low density, (d) medium density, (e) high density.

Fig. 2 The schematic representation of the microscopic system. The microcirculation is directly penetrated and illuminated from the side by while lighting source, the green channel absorbed by hemoglobin of erythrocytes which are observed as dark moving cells. The data analysis flow-chart was also shown in this illustration.

Fig. 3 A flowchart of velocity computation. Measurement of blood flow dynamics by an approach on the basis of optical flow estimation was shown in the schematic representation.

Fig. 4 (a) the image pixel matrix (1 mm^2) is 720 × 480 pixels. The rectangular region is selected as ROI's position (256 × 256 pixels). First image frame (b) and last image frame(c) are show in illustration, wherein the arrowhead indicates the direction of blood flow in microvessel. (d) Estimated 2-D blood flow velocity map that correspond to two image frames.

Fig. 5 An illustration of the weekly tumor growth on the back leg muscle of SCID mice.

Fig. 6 Weekly measured average tumor volume.

Fig. 7 Weekly measured average micro-vessel size.

Fig. 8 Averaged blood flow velocity at different weeks. Test of significance (independent T-test) value was indicated with a symbol “*” ($p<0.05$) in this illustration.

Fig. 1

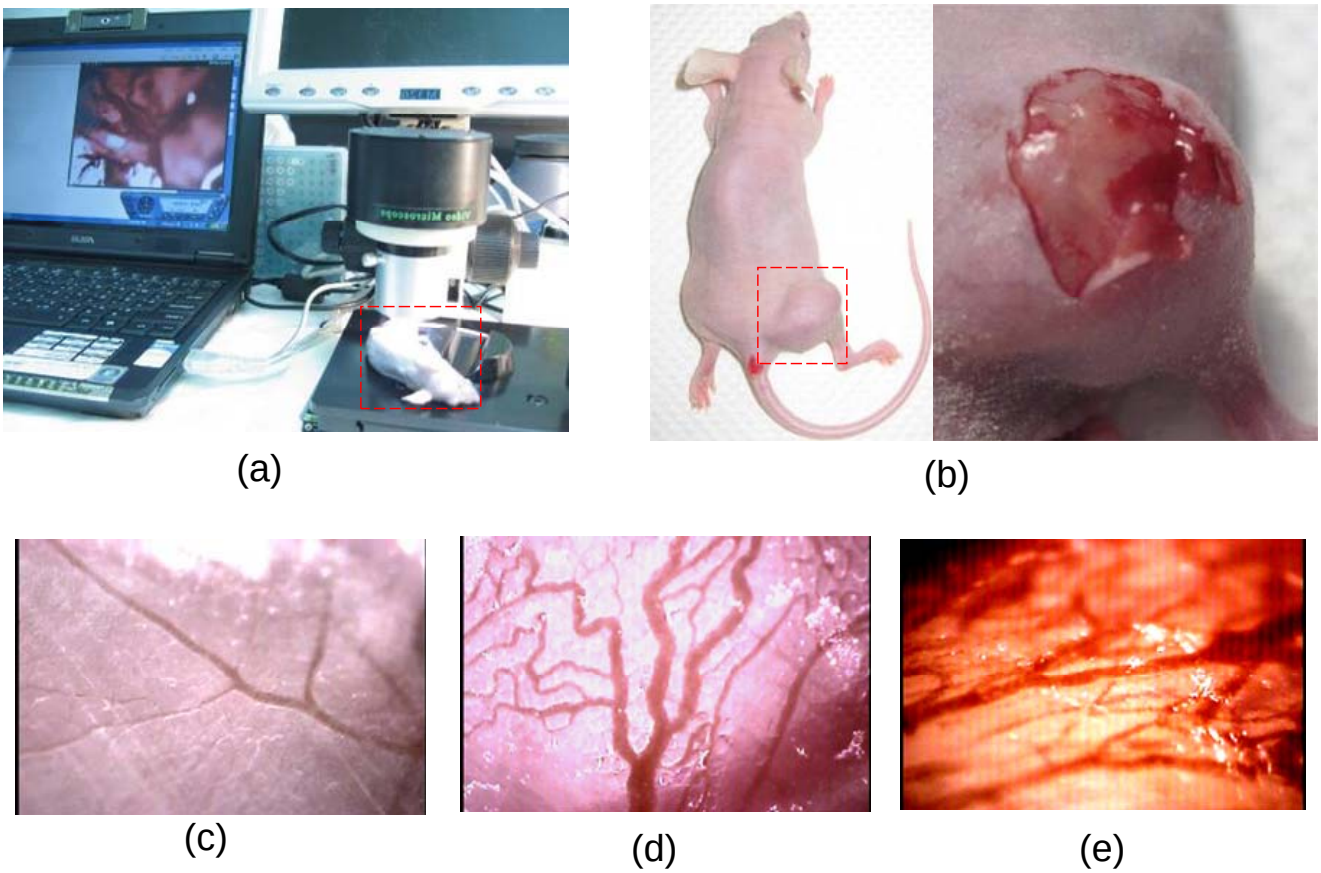
(a)
(b)
(c)
(d)
(e)

Fig. 2

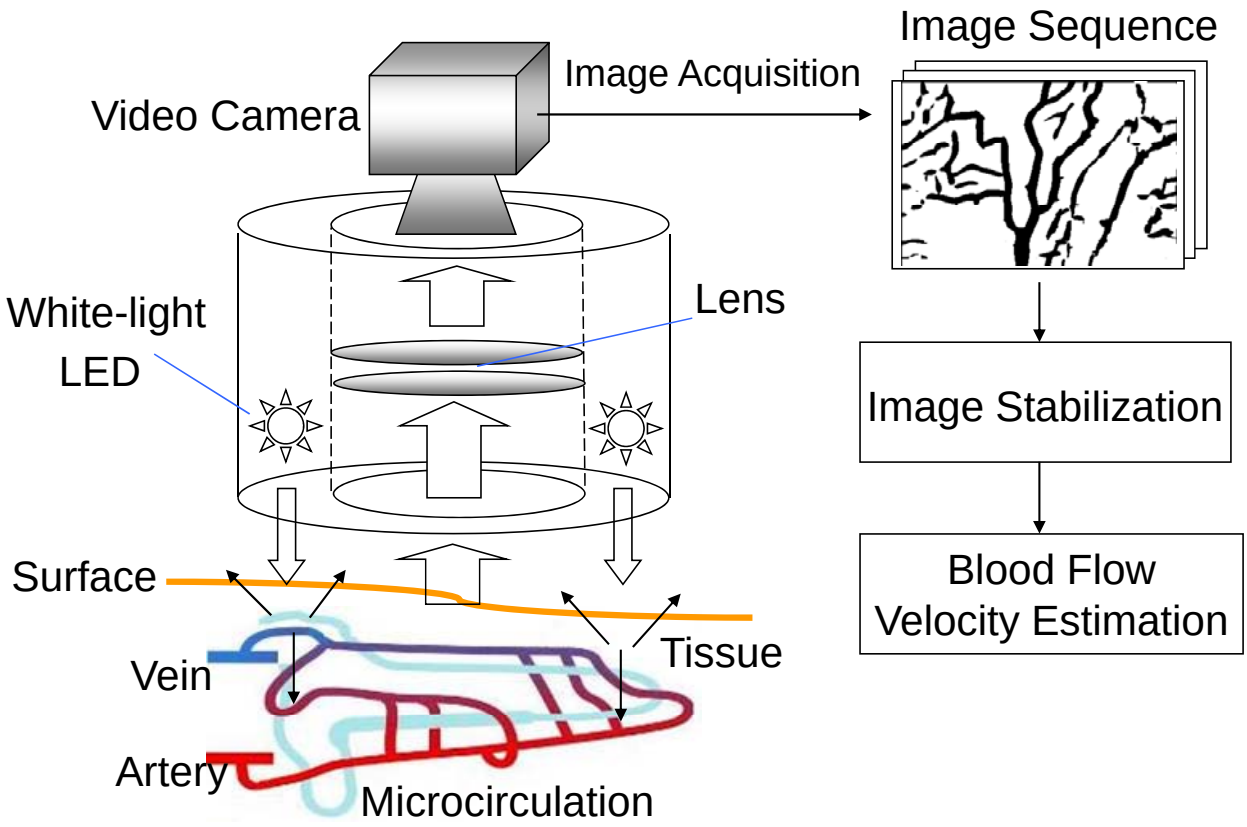
Image Sequence
Image Acquisition
Video Camera
Lens
White-light
LED
Image Stabilization
Blood Flow
Velocity Estimation
Surface
Tissue
Vein
Artery
Microcirculation

Fig. 3

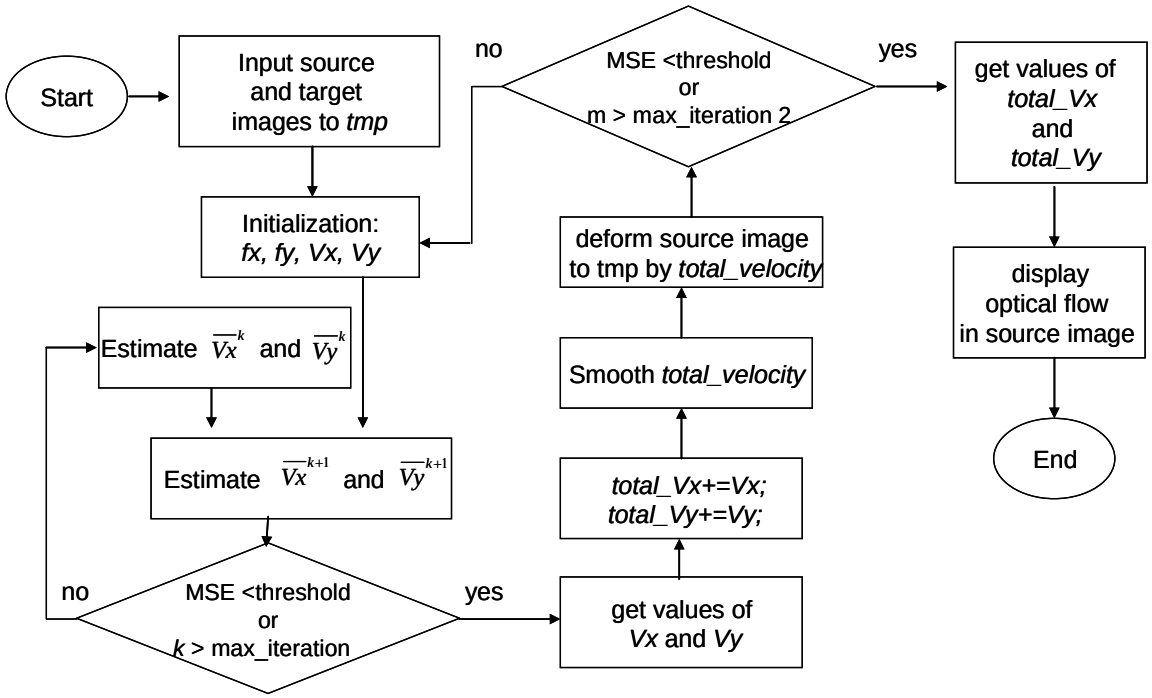

Fig. 4

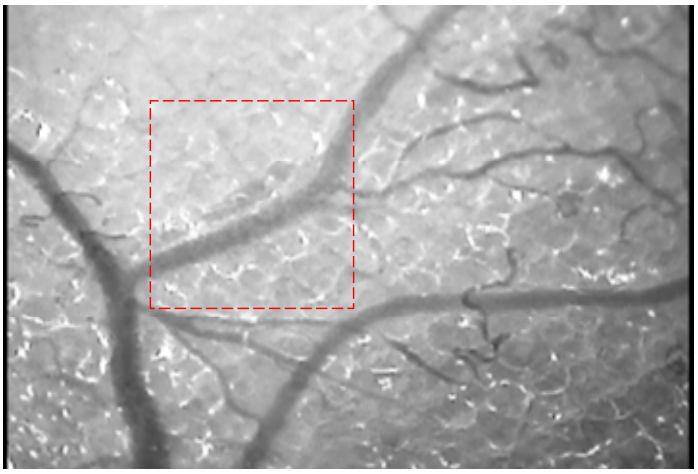

(a)

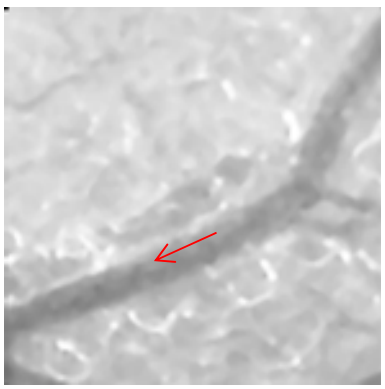

(b)

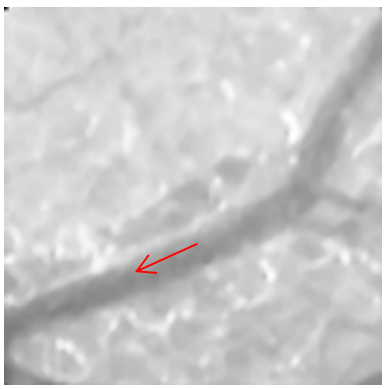

(c)

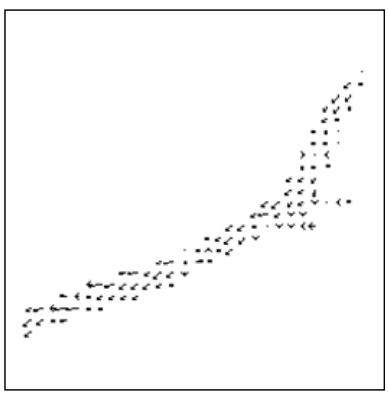

(d)

Fig. 5

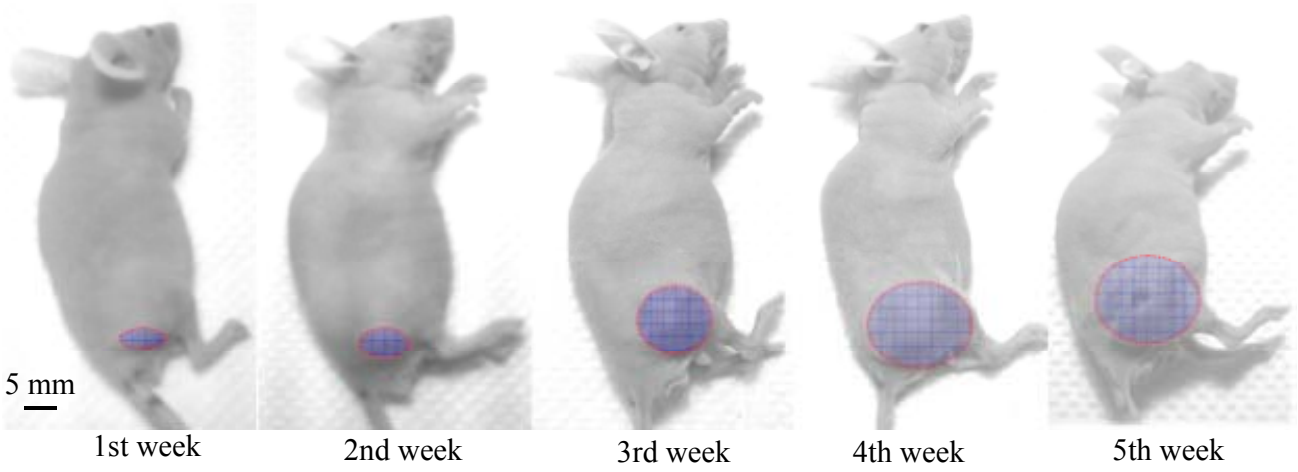
5 mm
1st week
2nd week
3rd week
4th week
5th week

Fig. 6

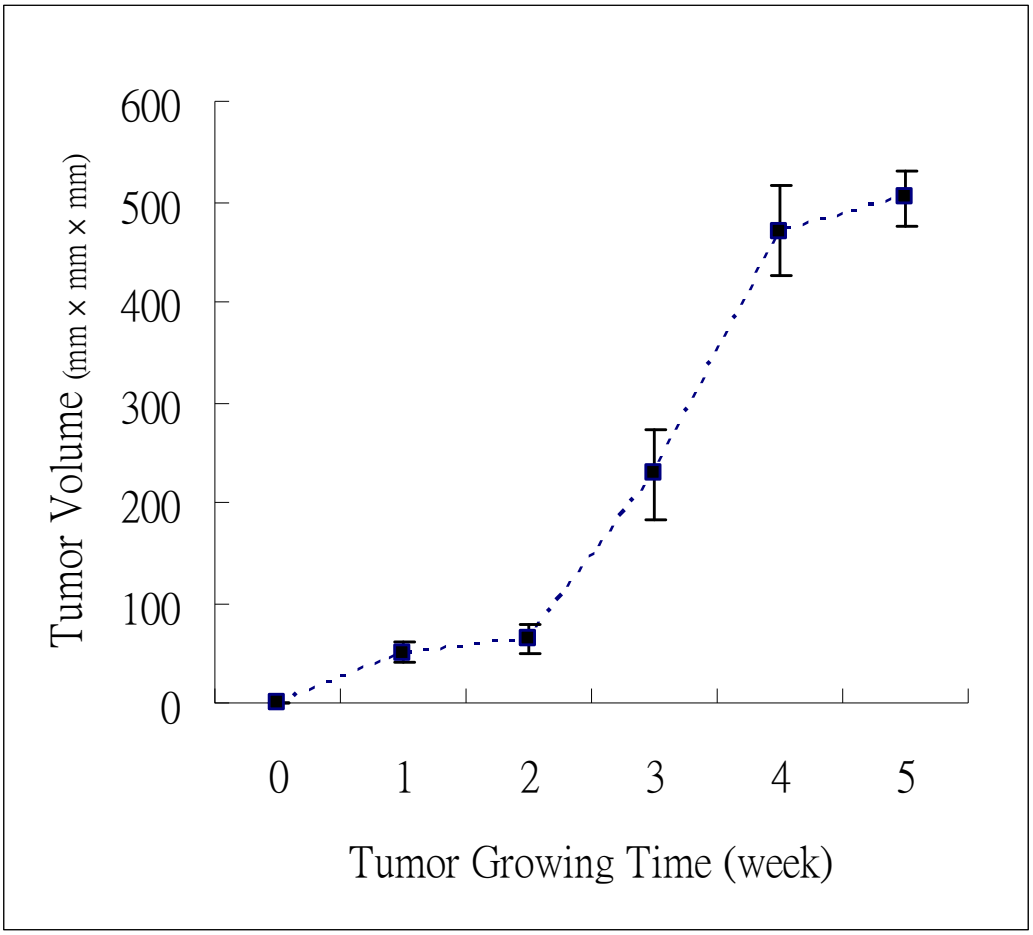
600
500
400
300
200
100
0
Tumor Volume (mm × mm × mm)
0
1
2
3
4
5
Tumor Growing Time (week)

Fig. 7

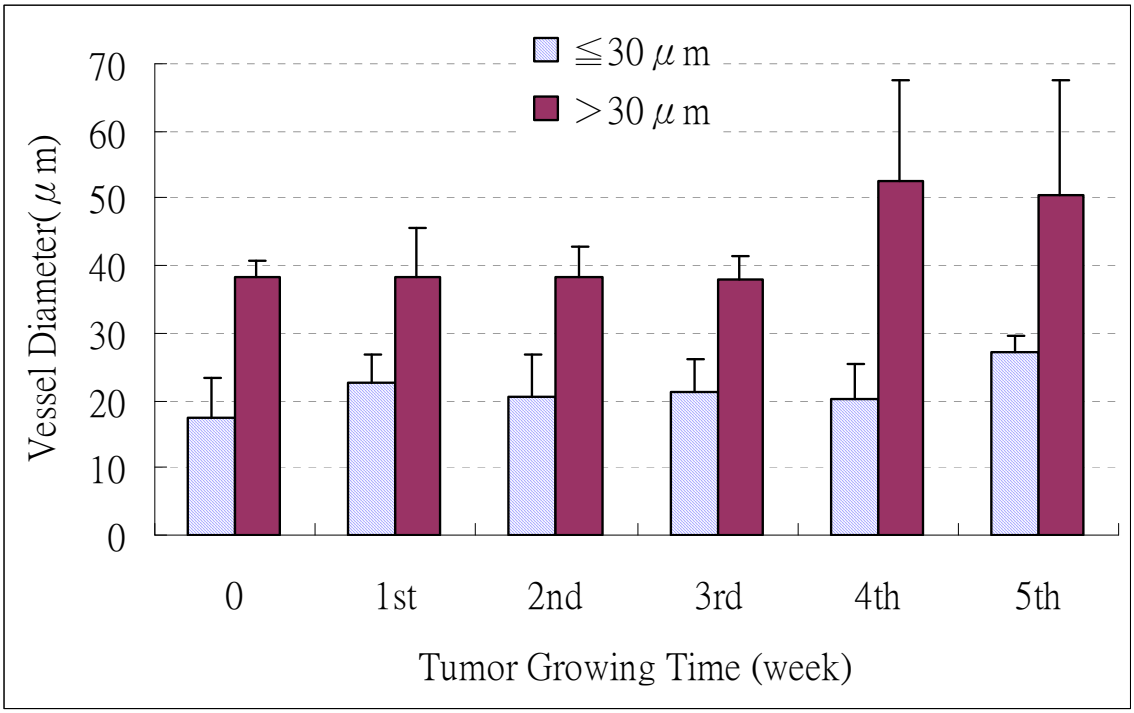
≦30 μm
>30 μm
Vessel Diameter(μm)
70
60
50
40
30
20
10
0
0
1st
2nd
3rd
4th
5th
Tumor Growing Time (week)

Fig. 8

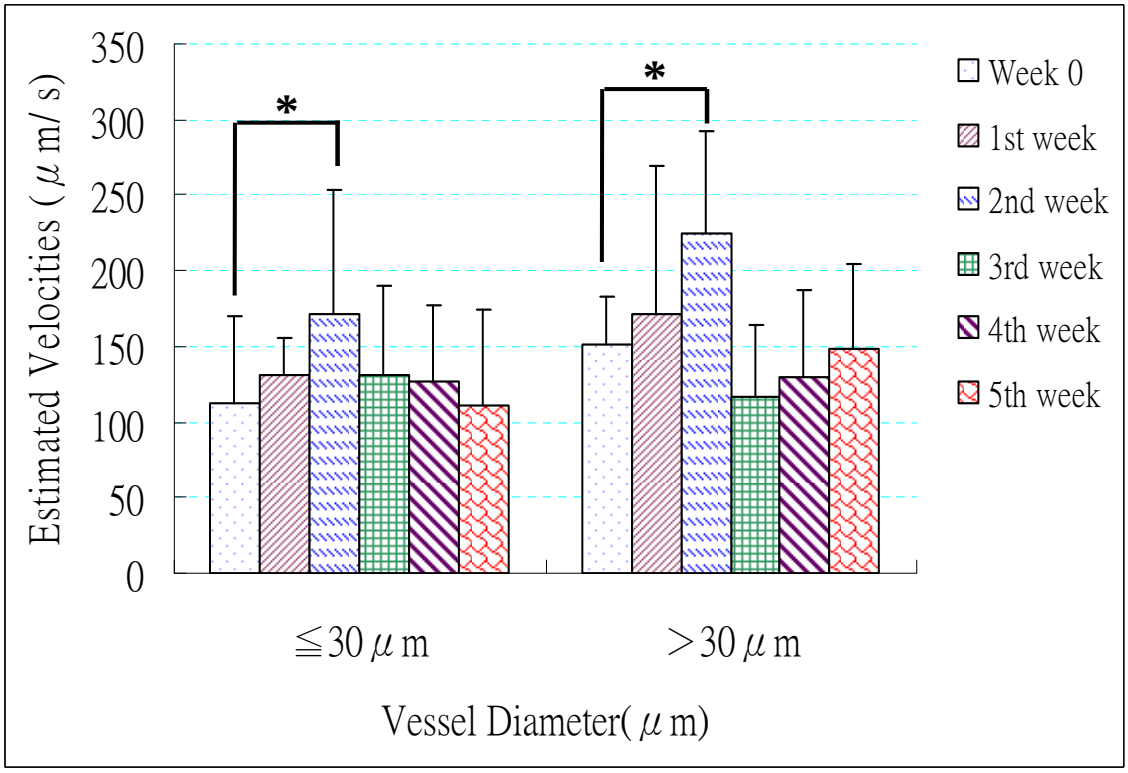
Estimated Velocities (μm/s)
350
300
250
200
150
100
50
0
*
*
Week 0
1st week
2nd week
3rd week
4th week
5th week
≦30 μm
>30 μm
Vessel Diameter(μm)